We are IntechOpen, the world's leading publisher of Open Access books Built by scientists, for scientists

4,800
Open access books available

122,000
International authors and editors

135M
Downloads

Our authors are among the

154
Countries delivered to

TOP 1%
most cited scientists

12.2%
Contributors from top 500 universities

CLARIVATE ANALYTICS BOOK CITATION INDEX INDEXED

WEB OF SCIENCE™

Selection of our books indexed in the Book Citation Index in Web of Science™ Core Collection (BKCI)

Interested in publishing with us?
Contact book.department@intechopen.com

Numbers displayed above are based on latest data collected.
For more information visit www.intechopen.com

5

Precipitates of γ–$Mg_{17}Al_{12}$ Phase in AZ91 Alloy

Katarzyna N. Braszczyńska-Malik
Institute of Materials Engineering
Technical University of Częstochowa
Poland

1. Introduction

Magnesium alloys are light metallic structural materials with a unique combination of properties, which are very attractive in such applications as the automobile, aerospace and electronic industries (Mordike & Ebert, 2001). The use of magnesium alloys has become significant due to a one-third lower density of magnesium compared with aluminium, improved damping ability, a higher resistance to corrosion and better mechanical properties. In lightweight magnesium alloys, aluminium constitutes the main alloying element, chiefly because of its low price, availability, low density and the advantageous effects on corrosion and strength properties (Smola et al., 2002). The AZ91 alloy (contains about 9 wt.% Al and 1 wt.% Zn, with addition of about 0.4 wt.% Mn) is the most widely used magnesium alloy exhibiting a good combination of high strength at room temperature, good castability and excellent corrosion resistance. According to the phase diagram (Fig. 1) the microstructure of Mg–Al alloys is generally characterized by a solid solution of aluminium in magnesium (an α phase with a hexagonal closely-packed, hcp structure) and the γ-phase.

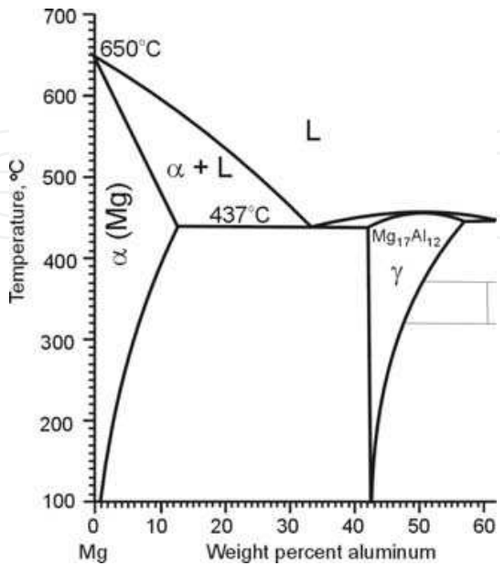

Fig. 1. Fragment of Mg–Al phase diagram (adopted from (ASM Handbook Committee, 1986))

The γ-phase (called also β-phase) is an intermetallic compound with a stoichiometric composition of $Mg_{17}Al_{12}$ (at 43.95 wt.% Al) and an α-Mn–type cubic unit cell. Young modulus of γ-phase is about 80 GPa whereas for magnesium only 45 GPa. In comparison with binary Mg–Al, new phases do not appear in commercial ternary alloys with zinc (like AZ91) when the Al to Zn ratio is larger then 3:1. In this case, the zinc substitutes aluminium in the γ-$Mg_{17}Al_{12}$ phase, creating a ternary intermetallic compound $Mg_{17}Al_{11.5}Zn_{0.5}$ or $Mg_{17}(Al,Zn)_{12}$ type (Braszczyńska-Malik K.N., 2005; Bursik & Svoboda, 2002 ; Celotto, 2000; Gonzalez-Martinez et al., 2007; Gharghouri et al., 1998; Celotto & Brastow, 2001).

2. The γ phase in as-cast AZ91 alloy

According to the equilibrium phase diagram, in Mg-Al alloys (Al concentration to 12.9 wt.%) after solidification process only one α-phase should occur. Non-equilibrium solidification condition cause the formation of large crystal of the primary γ-phase, depleted in alloying elements, and pushing the Al admixture away into interdendritical spaces. At the last stage of solidification the α + γ binary eutectic is formed at 473 K. In Mg-Al alloys eutectic can be fully or partially divorced dependent on aluminum content and solidification condition. Solidification conditions during gravity cast of magnesium alloys are effective in microstructure of casts. Differences in characteristic temperatures obtained during solidification of AZ91 alloy in cold steel and sand modulus (rod samples with a 200 mm diameter) are given in Fig. 2. Results were obtained from derivative thermal analysis (DTA) carried out by using a Cristaldigraph PC computer recorder. DTA curves were collected from thermocouple NiCr-NiAl with a 1.5 mm diameter, located directly into moulds. Measurements were archived with a sampling time of 0.2 s for steel mould and 1 s for sand mould. According to presented DTA results in a steel mould the AZ91 alloy solidified only 15 seconds whereas in sand mould (at the same size) about 680 seconds (Braszczyńska-Malik & Zyska, 2010).

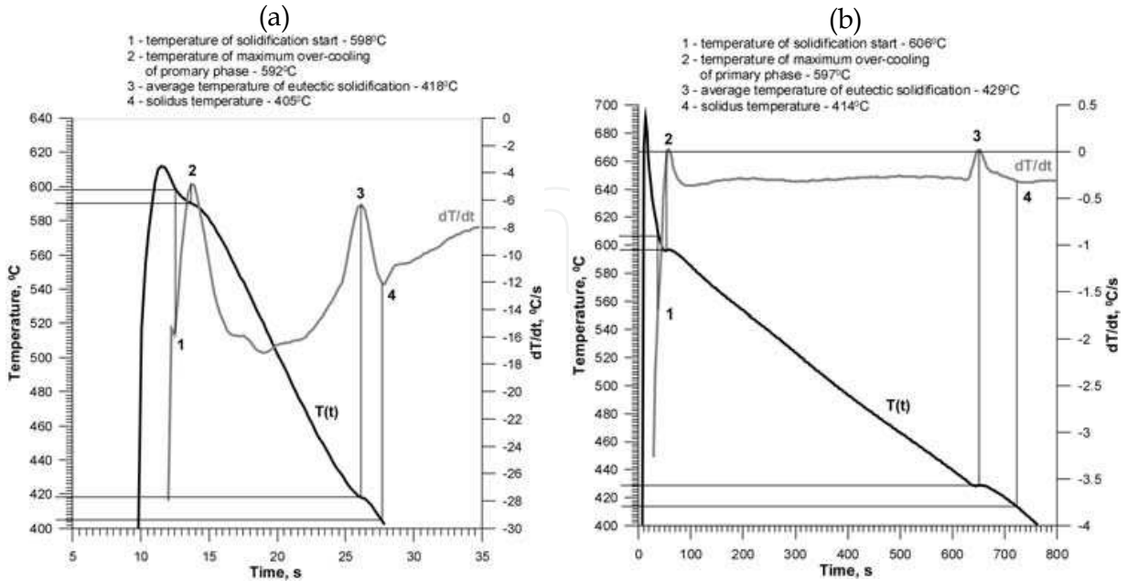

Fig. 2. DTA results: solidification curve T(t) and their first derivative dT/dt obtained for AZ91 alloy solidified in a steel (a) and sand mould (b)

Fig. 3 and 4 show microstructure of AZ91 magnesium alloy solidified in steel and sand moulds, respectively (rod samples with a 200 mm diameter). In both cases, the dendritical microstructure is characterised by the presence of α solid solution and the binary α + γ eutectic. Dendrite arms space (DAS) is visible high for alloy solidified in a sand mould. For samples cast into a steel mould, central areas of dendrites were strongly depleted in aluminium whereas near eutectic regions aluminium concentration was higher (Fig. 3b). Such aluminium distribution is very often observed in gravity cast AZ91 alloy. Differences in alloying elements distribution in microstructure were presented in Fig. 5 as the results of SEM+EDX analysis. Additionally, the presence of a small amount of manganese in commercial magnesium-aluminium alloys additionally causes the formation of aluminium-manganese intermetallic compounds Al_8Mn_5 or $Al_{11}Mn_4$ (Fig. 3b) (Braszczyńska-Malik K.N., 2005; Ohno et al., 2006).

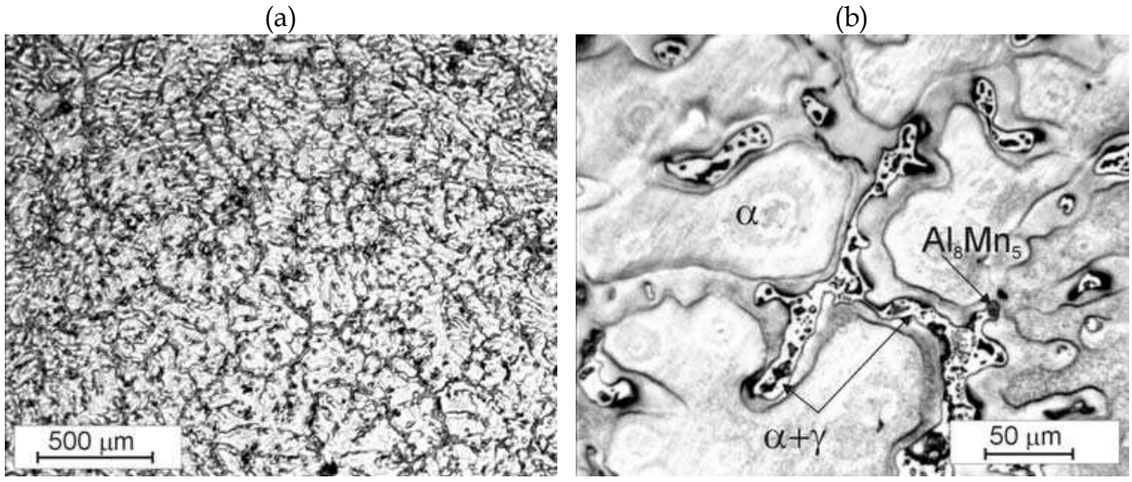

Fig. 3. Microstructure of AZ91 alloy; cast into a steel mould; light microscopy

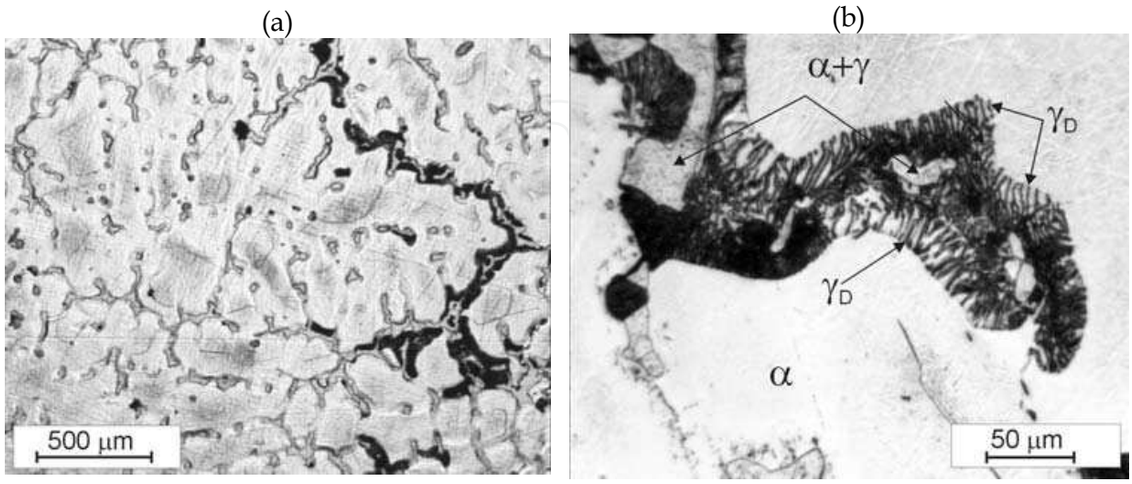

Fig. 4. Microstructure of AZ91 alloy; cast into a sand mould; light microscopy
($γ_D$ – discontinuous precipitates)

In the case of the alloy solidified in a sand mould, dark areas observed in Fig. 3a constitute regions of γ-phase discontinuous precipitates. Discontinuous precipitates (γ_D) formed from supersaturated solid solution (like areas marked as 2 in Fig. 5) due to slow cooling down of casts below the solvus temperature. Discontinuous precipitates are typical for AZ91 magnesium alloy gravity casts into sand moulds, where cooling of cast is slow. Characteristic lamellar structure of plate-like γ-phase is shown in Fig. 4b.

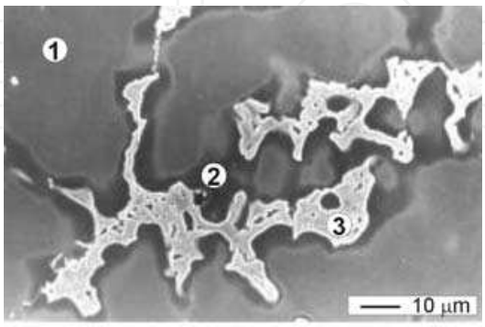

Point	Element	wt.%	at.%
1	Mg	95.03	95.50
	Al	4.97	4.50
2	Mg	90.10	91.27
	Al	9.33	8.52
	Zn	0.57	0.21
3	Mg	61.67	65.77
	Al	33.73	32.41
	Zn	4.60	1.82

Fig. 5. SEM image of AZ91 alloy; cast into a steel mould (a) and EDX analysis from points marked in the SEM image (b)

Analogical microstructure is observed in high-pressure die casts of Mg-Al alloys. Fig. 6 shows microstructure of AZ91 alloy from cast obtained using an Idra cold chamber machine (320 tone locking force). The microstructure consists of primary α phase and α + γ partially divorced eutectic (Braszczyńska-Malik et al., 2008).

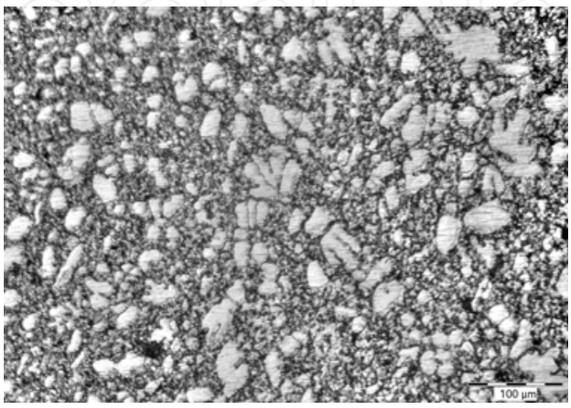

Fig. 6. Microstructure of AZ91 alloy; high-pressure die-casting; light microscopy

3. The γ phase in AZ91 alloy after heat treatment (discontinuous and continuous precipitation)

Magnesium-aluminium alloys are susceptible to heat treatment due to the variable solubility of their alloying elements in a solid state with temperature (Fig. 1). The maximum solid solubility of aluminium in magnesium is reasonably high at 12.9 wt.% Al at an eutectic temperature of 710 K whereas the equilibrium concentration at 473 K is about 2.9 wt.% Al. Solution annealing of the AZ91 alloy at 693 K caused a total dissolution of the α+γ eutectic and homogenised the aluminium throughout the matrix. The time necessary to obtain the homogeneous microstructure consisting of solid solution grains is very long (minimum 24 h) due to very slow diffusion of aluminium in a magnesium solid state. It should also be noted, that the Al_8Mn_5 intermetallic compound is not involved in heat treatment (Braszczyńska-Malik, 2009 a). The microstructure obtained after solution annealing is shown in Fig. 7.

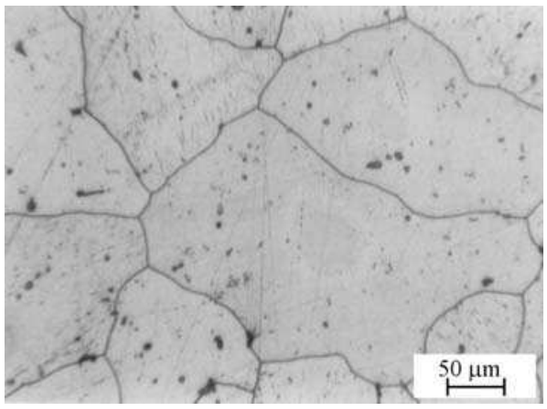

Fig. 7. Microstructure of AZ91 alloy after solution annealing at 693 K for 24 h; light microscopy

During conventional heat treatment, involving solution annealing at about 690 K for a minimum of 24 h, followed by ageing at about 430 K for 16 h (T6 conditions), the precipitation process appears and the formation of γ phase precipitates occurs. During γ phase precipitation, neither Gunier-Preston zones nor other metastable phases are formed (Dully et al. 1995). The microstructure of the AZ91 alloy after ageing of the supersaturated solid solution at 423 K for 16 h (T6 conditions) is characterized by the presence of fine, plate-like, discontinuous γ precipitates. Fig. 8 shows a typical microstructure of the AZ91 alloys after this heat treatment. The γ phase precipitates had a lamellar morphology with a marked anisotropy of growth.

However, precipitation occurring in supersaturated alloys can take place either continuously or discontinuously. During both discontinuous and continuous precipitation reactions, representing a solid-solid phase transformation, a supersaturated solid solution (α_0) decomposes into a new solute-rich precipitate (γ) and a less-saturated, near-equilibrium, initial phase (α) with the same crystal structure as the α_0. The differences between discontinuous and continuous precipitation consist in the nucleation places and growth. Discontinuous precipitation (DP) is the cellular growth of alternating plates of the secondary phase and near-equilibrium matrix phase at high angle boundaries. This heterogeneous reaction leads to the formation of a lamellar structure behind a moving grain boundary.

Continuous precipitation (CP) proceeds by a different mechanism, where precipitates of the γ phase nucleate and grow inside the α_0 grains. In most alloys, nevertheless, these two types of precipitates can also occur simultaneously (Braszczyńska, 2002; Cerri & Barbagallo, 2002; Bradai et al., 2001; Bettles, 2003; Nie et al., 2001).

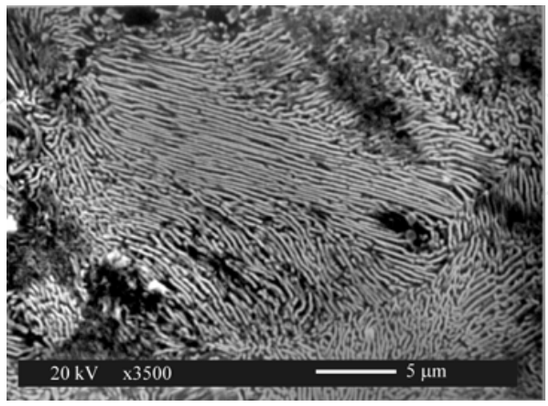

Fig. 8. Discontinuous precipitates in AZ91 alloy after ageing supersaturated solid solution at 423 K for 16 h; SEM

Figs. 9-10 show typical SEM images representing the variation in precipitation morphology with the temperature. At the temperature of 545 K both continuous and discontinuous precipitates were observed. The light areas in Fig. 9a represent typical colonies of discontinuous lamellar precipitates growing from the grain boundaries. Additionally, after ageing at this temperature, small continuous precipitates inside the grains were observed. Fig. 9b illustrates fine continuous precipitates observed after ageing for 2 h at 545 K. The same results were obtained after ageing at 473 K and 543 K for binary Mg-9 wt.% Al alloy (Braszczyńska-Malik, 2009 a).

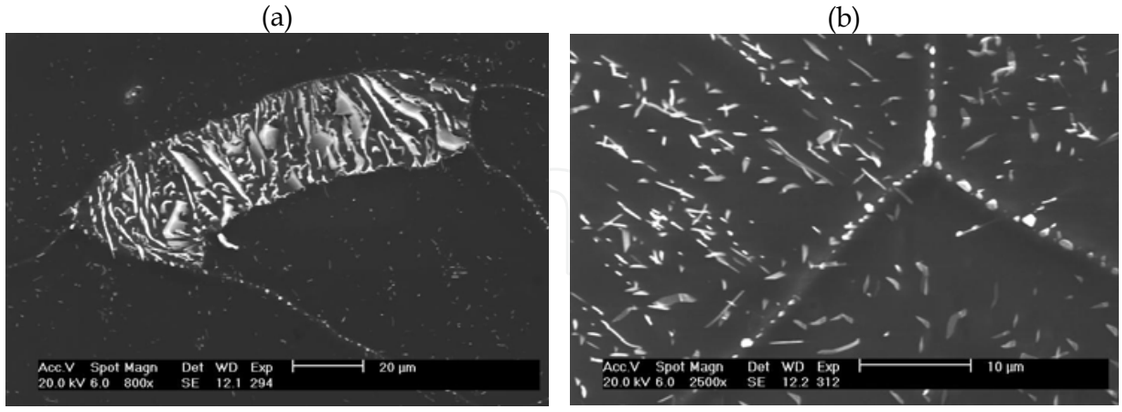

Fig. 9. Discontinuous (a) and continuous (b) precipitates of γ phase in AZ91 alloy after ageing at 545 K; SEM

A different situation was observed after ageing supersaturated alloys at 623 K. Although in the samples aged for 1 h the presence of γ precipitates at the grain boundaries was also revealed (Fig. 10a), the process of its growth was quickly stopped. Ageing of the AZ91 alloy at 623 K for 2 h caused the occurrence only of continuous precipitates also with a visible

orientation relationship with the matrix grains (Fig. 10b). It should be noted, that at this temperature (623 K) typical colonies of discontinuous precipitates did not occur. The same results were observed for the binary Mg-9 wt.% Al alloy (Braszczyńska-Malik, 2009 a).

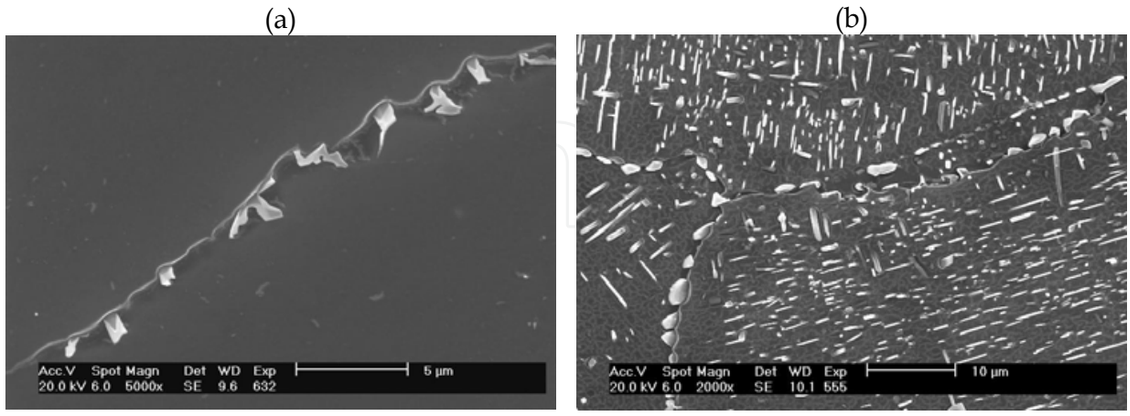

Fig. 10. Precipitates of γ phase at grain boundary (a) and continuous precipitates (b) in AZ91 alloy after ageing at 623 K; SEM

As was revealed, for the AZ91 alloy, discontinuous and continuous precipitates can occur simultaneously or competitively, dependently on the ageing temperature. After ageing at 423 K typical colonies of discontinuous precipitates were observed whereas at 623 K only continuous precipitates were formed inside grains. It proved that continuous precipitation tends to be favoured at high temperatures (i.e. close to the solvus curve) whereas at low temperatures of ageing, discontinuous precipitation invades all the samples. The presented observations also indicate that at an intermediate temperature range both discontinuous and continuous precipitates can be observed. The same results were obtained for the commercial AZ91 alloy and experimentally binary Mg-9 wt.% Al alloy (Braszczyńska-Malik, 2009a). It confirmed, that zinc present in the commercial alloy not does influence the precipitate type. It should also be noted, that the volume fraction of continuous precipitates increased with ageing temperature. Nevertheless, the mutual ratio of the discontinuous and continuous precipitates in each sample is practically not evident, because it depends on the local conditions for nucleation and growth in the grains and at grain boundaries. Additionally, as could be expected, the time necessary for nucleation and growth of precipitates decreases with ageing temperature. As well known, the volume fraction of regions transformed by discontinuous precipitation essentially depend on reaction front velocity, interlamellar spacing, average composition of the solute-depleted α lamellae, temperature, solute content and conditions of the grain boundaries (Bradai et al., 2001; Bradai et al. 1999; Braszczyńska 2002; Maitrejean et al., 1999; Zięba, 2000). The phase transformation during continuous precipitation is mainly described as the sequential or simultaneous processes of nucleation, growth and impingement (Celotto, 2000; Celotto & Bastow 2001; Duly et al. 1995). In both cases, reduction of the driving force for propagation and impediment of nucleation may be the limiting factors. However, a simple dependence describing the dominant type of precipitation did not seem to exist. It should also be noted, that at all temperatures, grain boundaries tend to be rapidly decorated by arrays of heterogeneous γ precipitates testifying that the grain boundaries are the first and privileged places of nucleation for precipitates.

Additionally, the amount of continuous precipitates very strongly depends on the number of crystal defects within the matrix which may act as heterogeneous nucleation sides. It well known, that besides the grain boundaries, the various nucleation sizes are: vacancies, dislocations, stacking faults and solid free surfaces. One possibility is the heterogeneous nucleation of continuous precipitates on vacancies. On the other hand, vacancies also determine the volume diffusion mechanism. Due to comparable Al and Mg atom diameters, vacancy diffusion can be dominant in the investigated alloys. Solution annealing and quenching result in a higher (non-equilibrium) vacancy concentration. If a concentration of vacancy is lower (i.e. near-equilibrium) continuous precipitates of the γ phase cannot occur.
As expected for a higher temperature the diffusion became faster, resulting in an increase of volume precipitates. Moreou et al. (1971) have found that the volume diffusion coefficient (D_V) for aluminium in magnesium can be determined using:

$$D_V = 12x10^{-4} \exp\left(\frac{-144x10^3}{RT}\right) \quad \mathrm{m}^2/\mathrm{s} \tag{1}$$

Discontinuous precipitation is described by Sundquist, Cahn, Hillert, Turnbull or Petermann-Hornbogen models (Bradai et al., 1999; Maitrejean et al., 1999) whereas continuous precipitation by the Austin and Ricket (A–R) equation or the well-known Avrami equation, which is also known as the Johnson–Mehl–Avrami–Kolmogorov (JMAK) equation (Celotto, 2000). For consistency, the grain boundary diffusivities for discontinuous precipitation can be evaluated using the Petermann-Hornbogen equation (Bradai et al., 1999; Zieba, 2000):

$$s\delta D_{gb} = \frac{RT}{-8\Delta G}\lambda^2 \nu \tag{2}$$

where D_{gb} is the grain boundary diffusion coefficient, δ - the grain boundary width, s - the segregation factor, ν - the velocity for the process, ΔG - the total driving force, R - the gas constant, T - the absolute temperature of the process and λ is the interlamellar spacing.
Bradai et al. (1999) has determined the Arrhenius parameters as the pre-exponential factor $(s\delta D_{gb})_0 = 1.15x10^{-6}$ m^3/s and the activation energy for grain boundary diffusion: $Q_{gb} = 105.3$ kJ/mol. A different value of $Q_{gb} = 128$ kJ/mol was reported by Amir & Gupta (1995). On the other hand, the grain boundary diffusion coefficient, D_{gb}, can be calculated from equation (2) assuming s = 1 and δ = 0.5 nm, according to (Bradai et al., 1999). In Fig. 11 the diffusion coefficients, D_v (from equation (1)) and D_{gb} (from equation (2) where the pre-exponential factor ($s\delta D_{gb}$) was evaluated from the Arrhenius plot) were presented. The obtained values show that the volume diffusion coefficient is approximately 6-7 orders of magnitude less than the diffusion coefficient for the grain boundary. At lower temperatures the process of secondary precipitation is controlled by grain boundary diffusion. It causes discontinuous precipitates to form earlier at the grain boundaries in characteristically shaped colonies of lamellae. As the temperature increases, bulk diffusion becomes faster, which tends to favour continuous precipitation. Continuous precipitation reduces the amount of chemical driving energy available for both the initiation and propagation of discontinuous precipitates. So if the continuous precipitation process started inside the grains then discontinuous precipitates are stopped.

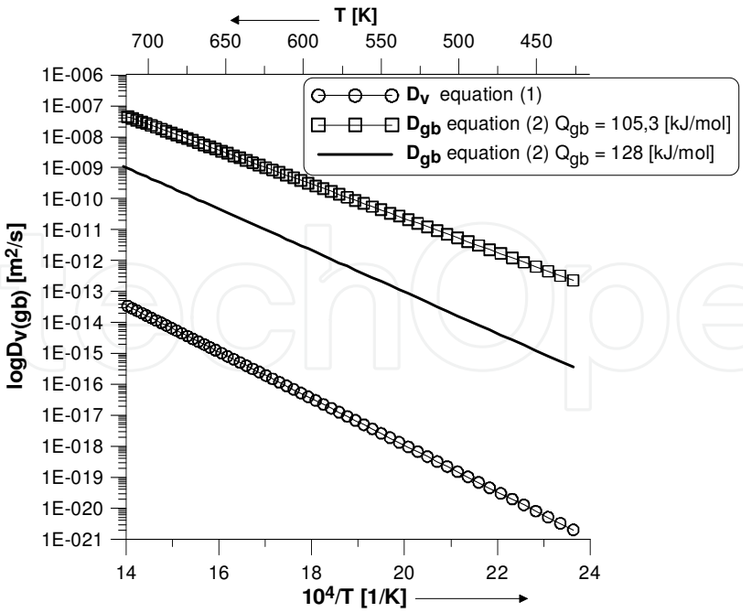

Fig. 11. Volume (D_V) and grain boundary (D_{gb}) diffusion coefficient for aluminium in magnesium based on [19, 25, 27] data

For both precipitates, the predominant orientation relationship (OR) is the Burgers OR, namely: $(0001)_\alpha \parallel (0\,\bar{1}\,0)_\gamma$ and $[2\,\bar{1}\,\bar{1}\,0]_\alpha \parallel [111]_\gamma$ (Braszczyńska-Malik, 2005; Celotto & Bastow, 2001; Zhang et al., 2003). Additionally, other ORs were also reported in Mg-Al based alloys, i.e. the Crawley OR (Celotto, 2000; Gharghouri et at., 1998), the Porter OR (Celotto, 2000), the Gjömmes-Östrmoe OR (Zhang et al., 2003; Nie et al., 2001) or the Potter OR (Nie et al., 2001; Bradai et al. 1999).

Precipitates with the Burgers OR are parallel to the basal plane of the matrix, i.e. $(0001)_\alpha$ whereas precipitates with optional ORs lie on the prism plane of the magnesium i.e. $(1\,\bar{1}\,00)_\alpha$ and they are perpendicular to the basal plane of the matrix. The strain caused by the γ phase precipitate may be seen clearly from its eigenstrain matrix. In this case, the hcp α phase must be transformed to a regular cubic γ phase. During transformation, the coordinates system of matrix $x_1^\alpha - x_2^\alpha - x_3^\alpha$ must be changed to the coordinates of precipitate $\xi_1^\gamma - \xi_2^\gamma - \xi_3^\gamma$. Fig. 12 shows a scheme of the transformation α phase to the γ precipitate according to the Burgers OR and the Crawley OR. Transformations for the Porter OR and the Gjömmes-Östrmoe OR are analogical to those presented for the Crawley OR.

The lattice deformation matrix A to change the α lattice into the γ lattice can be written as:

a. for the Burgers OR:

$$A^{\rightarrow B} = \begin{pmatrix} \frac{a_\gamma\sqrt{3}}{\kappa a_\alpha} & 0 & 0 \\ 0 & \frac{\sqrt{11}a_\gamma}{3\kappa a_\alpha\sqrt{3}} & 0 \\ 0 & 0 & \frac{a_\gamma\sqrt{2}}{\kappa c_\alpha} \end{pmatrix} - \delta_{ij} \tag{3}$$

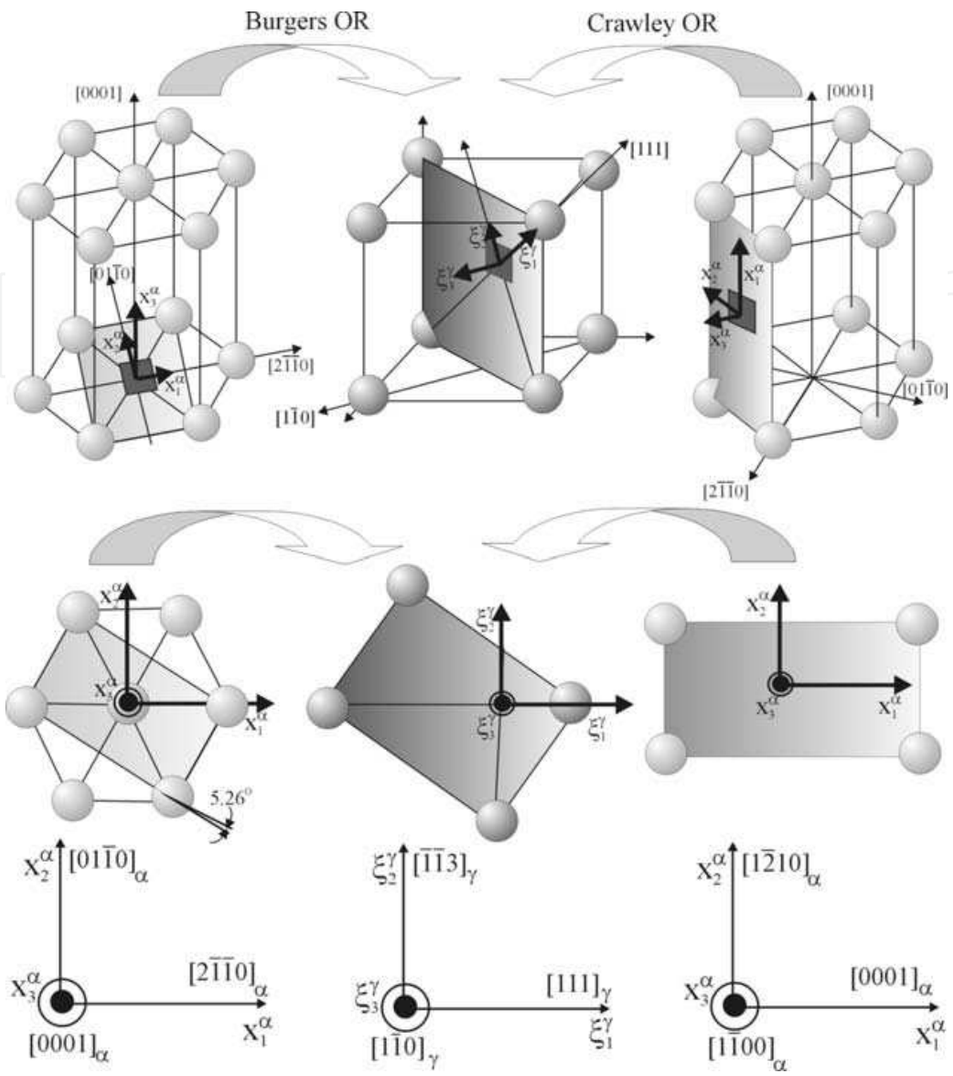

Fig. 12. Scheme of hcp α-phase matrix lattice transformation to γ precipitate lattice

b. for the Crawley OR:

$$A^{\rightarrow C} = \begin{pmatrix} \frac{a_\gamma\sqrt{3}}{\kappa c_\alpha} & 0 & 0 \\ 0 & \frac{a_\gamma\sqrt{3}}{\kappa a_\alpha\sqrt{2}} & 0 \\ 0 & 0 & \frac{a_\gamma\sqrt{2}}{\kappa a_\alpha\sqrt{3}} \end{pmatrix} - \delta_{ij} \tag{4}$$

where δ_{ij} is the Kronecker delta, a_α, c_α are the lattice parameters of the α phase, a_γ is the lattice parameter of the γ phase, and κ is a multiplication factor introduced due to the large difference in lattice parameters between the α and γ phase (Braszczyńska-Malik, 2005). Additionally, rigid-body rotation, δ_{ij}, by $\varpi = 5.26°$ is necessary to realize the Burgers OR:

$$\lambda_{ij} = \begin{pmatrix} \cos\varpi & -\sin\varpi & 0 \\ \sin\varpi & \cos\varpi & 0 \\ 0 & 0 & 1 \end{pmatrix} \tag{5}$$

Therefore, the total transformation matrix to include the change in the crystal structure becomes:

a. for the Burgers OR

$$\varepsilon_{ij}^{\xi \to B} = \begin{pmatrix} -0.0512 & -0.009 & 0 \\ -0.009 & 0.0472 & 0 \\ 0 & 0 & -0.046 \end{pmatrix} \tag{6}$$

b. for the Crawley OR

$$\varepsilon_{ij}^{\xi \to C} = \begin{pmatrix} -0.12 & 0 & 0 \\ 0 & 0.0053 & -0.0012 \\ 0 & -0.0012 & 0.0714 \end{pmatrix} \tag{7}$$

The obtained results suggest the presence of coherent boundaries with slight lattice deformation between the magnesium matrix and γ precipitates. It is known that the interphase boundary may be coherent if the lattice incoherence is less than 0.1. Low values obtained from transformation matrices (equation (6) and (7)) explain both plate-like morphology of precipitates and its visible anisotropy of growth.

4. The γ phase in AZ91 alloy after equal-channel angular pressing

The grain refinement is very important in magnesium alloys because they have poor formability and limited ductility at room temperature rooted in their hexagonal close-packed (hcp) crystal structure. In the past decade, efforts have been concentrated on thermomechanical processing for grain size refinement using methods of severe plastic deformation (SPD) (Valiev et al., 2000). SPD techniques, such as equal channel angular pressing (ECAP) (Valiev et al., 2000; Valiev & Langdon, 2006; Chen et al., 2008; Ravi Kumar et al., 2003; Wang et al., 2008), accumulative roll bonding (ARB) (Jiang et al., 2008; Saito et al., 1999) or high-pressure torsion (HCP) (Zhilyaev & Longdon, 2008; Zhiyaev et al., 2003), have been applied to the grain refinement of magnesium alloys on bulk materials. The influence of ECAP process on precipitation in AZ91 magnesium alloy was also investigated (Braszczyńska-Malik, 2009 b). The ECAP die used in the presented investigation was designed to obtain a maximum shear strain of about 1.15 during each pass. It contained an inner contact angle Φ equal to 90° and corner angle Ψ of 0°. The billets (with 11.8 mm of diameter and 50 mm of length) were processed at a pressing rate of 5 mm/min. using a plunger attached to a hydraulic press on an Instron machine. All the pressings were conducted using route B_C where the billet is rotated 90° (clockwise) around the lengthwise axis between each pass. For each separate pressing, the samples were coated with molybdenum disulphide (MoS_2) as a lubricant. AZ91 alloy was heat treatment before ECAP (solution annealing – 698 K, 24 h – Fig. 7)

Figs. 13 and 14 show microstructure of AZ91 alloy after 4 ECAP passes at 553 and 623 K. The presented results indicated that the microstructure of the AZ91 alloy processed by ECAP at 553 and 623 K via the B_C pressing route at a rate of 0.16 mm/s consisted of α matrix phase equiaxal grains of about 10 μm in size (Fig. 13) and spherical precipitates located particularly inside the grains (Figs. 13 and 14). The observed precipitates were unequivocally identified as the γ phase (Fig. 14). The microstructure observations carried out on both the transverse and the longitudinal sections of the pressed samples provides direct evidence of the spherical shape of precipitates with a maximum size of about 1 μm. It is well known that equilibrium morphology is a shape that minimizes the total energy which is composed of two parts: elastic strain energy and interfacial energy.

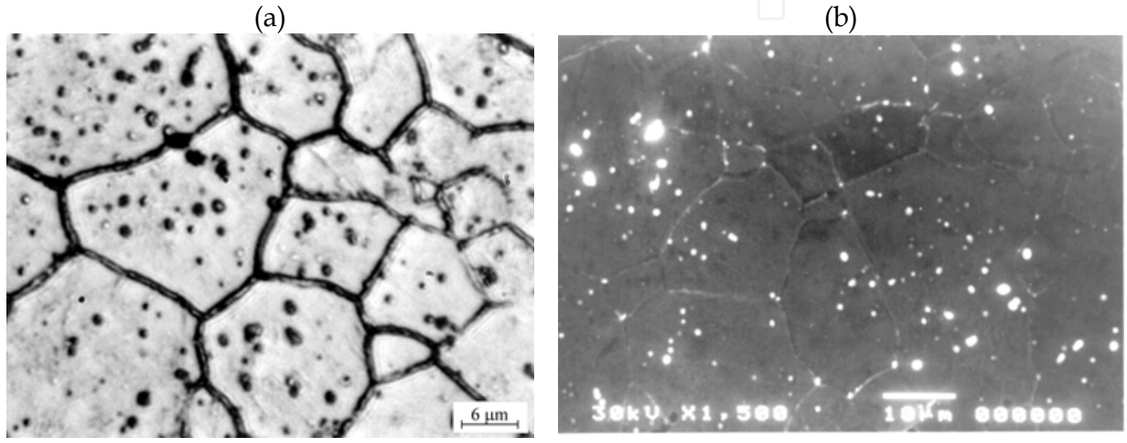

Fig. 13. Spherical precipitates of γ phase in AZ91 alloy after ECAP at 553 K; light microscopy (a), SEM (b)

On the other hand, the analysed planes (basal and prism planes) in hcp magnesium are simultaneously the main slip planes. For magnesium with a c/a ratio equal to 1.624 the main slip system is $\{0001\}\langle 11\bar{2}0\rangle$. It is well known that the three main dislocations determined as (i) **a** type with Burgers vector $1/3[11\bar{2}0]$, (ii) **c** type with Burgers vector 1/2[0001] and (iii) **c+a** type with Burgers vector $1/3[11\bar{2}\bar{3}]$ can operate in magnesium (Woo, 2000; Mathis et al., 2004). In case of unfavourable orientation of the main slip system to external stress or in higher temperatures, different slip systems e.g. $\{1\bar{1}00\}\langle 11\bar{2}0\rangle$ and $\{1\bar{1}01\}\langle 11\bar{2}0\rangle$ can also operate. In works concerning hot working of magnesium alloys (Koike et al. 2003; Yoo et al. 2001) however, an <a> cross slip and energetically favorable junction between glissile <a> and sensile **c** dislocations on a $\{1\bar{1}00\}$ prism plane seem to be predominant. The dissolution of an **a** dislocation on the basal plane to Shockley partial dislocations connected with a single stacking fault is also possible. However, plastic deformation during SPD processes especially of magnesium alloys at high temperatures appears to be more composite and complicated. For example, in the present case, the supersaturated solid solution exhibited higher than equilibrium solute atoms concentration, which could form atmospheres generating dislocation locking. It should also be noted that the deformation of hcp magnesium alloys caused the formation of twins, especially the $\{1\bar{1}02\}_{matrix} \,||\, \{0\bar{1}12\}_{twin}$ type (Christian & Mahajan, 1995; Braszczyńska- Malik et al., 2006).

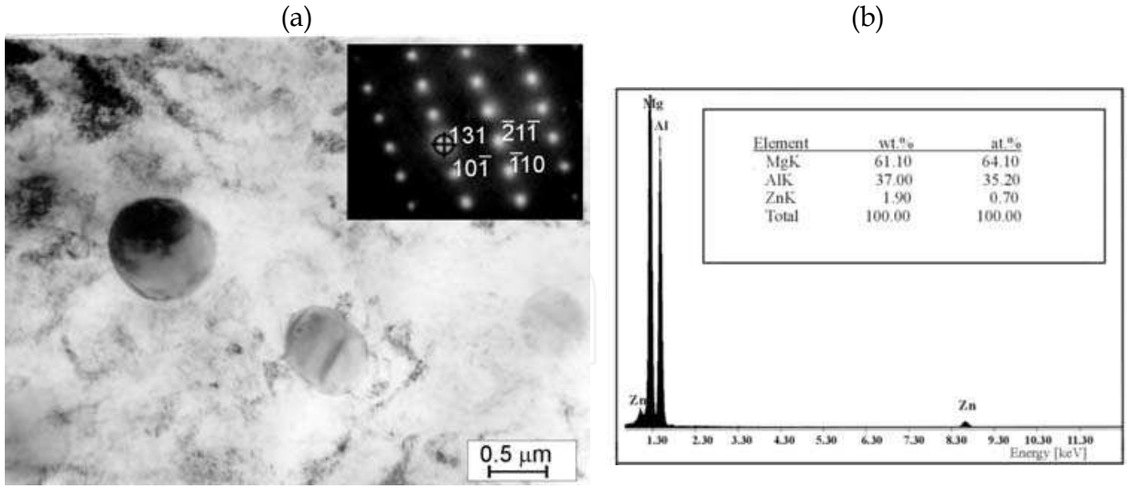

Fig. 14. TEM image of spherical precipitates of γ phase in AZ91 alloy after ECAP at 623 K (a), and result of EDX analysis obtained from one of precipitate (b)

In most published works (Janecek et al., 2007; Su et al., 2006; Kulyasova et al., 2009; Braszczyńska-Malik & Froyen, 2005; Braszczyńska- Malik et al., 2006) the microstructure of magnesium alloys processed by the ECAP technique was characterized by strong deformation and high density of dislocations and twins. Introducing a high dislocation density and strong disordering of the matrix lattice during severe plastic deformation can preclude formation of a coherent boundary between the matrix and growing γ precipitates. If precipitate growth proceeds during continuous plastic deformation, then the plate-like shape of precipitates is unfavourable. In this case the spherical shape of precipitates can be the most energetically favorable. On the other hand, the high density of crystal defects introduced inside α–phase grains during plastic deformation act as privileged sites for the heterogeneous nucleation of precipitates. Additionally, high dislocation density (and other defects like vacancies) caused faster diffusion of solute atoms in the magnesium matrix which were effective in reducing the time necessary for the nucleation and growth of precipitates (in comparison to precipitation during heat treatment). For this reason also, spherical precipitates were observed especially inside matrix grains which is clearly seen in Fig. 13.

In the present case, a new spherical shape of γ precipitates was obtained in the AZ91 alloy processed by ECAP at a maximum shear strain of about 1.15 during each pass and at a pressing rate of 0.16 mm/s. The applied ECAP parameters allowed the attainment of severe plastic deformation introducing strong disordering of the magnesium lattice. On the other hand, the temperature and time were suitable for the growth of precipitates during deformation. Thus, the selected process parameters allowed the attainment of new spherical precipitates of the γ phase.

7. Conclusion

1. In as-cast microstructure of AZ91 magnesium alloy the γ phase is mainly constituent of more or less divorced eutectic (but it should also be noted that in slow cooling down casts it my also creates discontinuous precipitates).

2. After ageing of supersaturated solid solution at 423 K only discontinuous precipitates are observed whereas at 623 K only continuous once are revealed in the microstructure of AZ91 alloy. At intermediate ageing temperatures both discontinuous and continuous precipitates of the γ phase occur.
3. The spherical shape of γ precipitates can be obtained due to correlate precipitation and magnesium matrix deformation processes (Fig. 15).

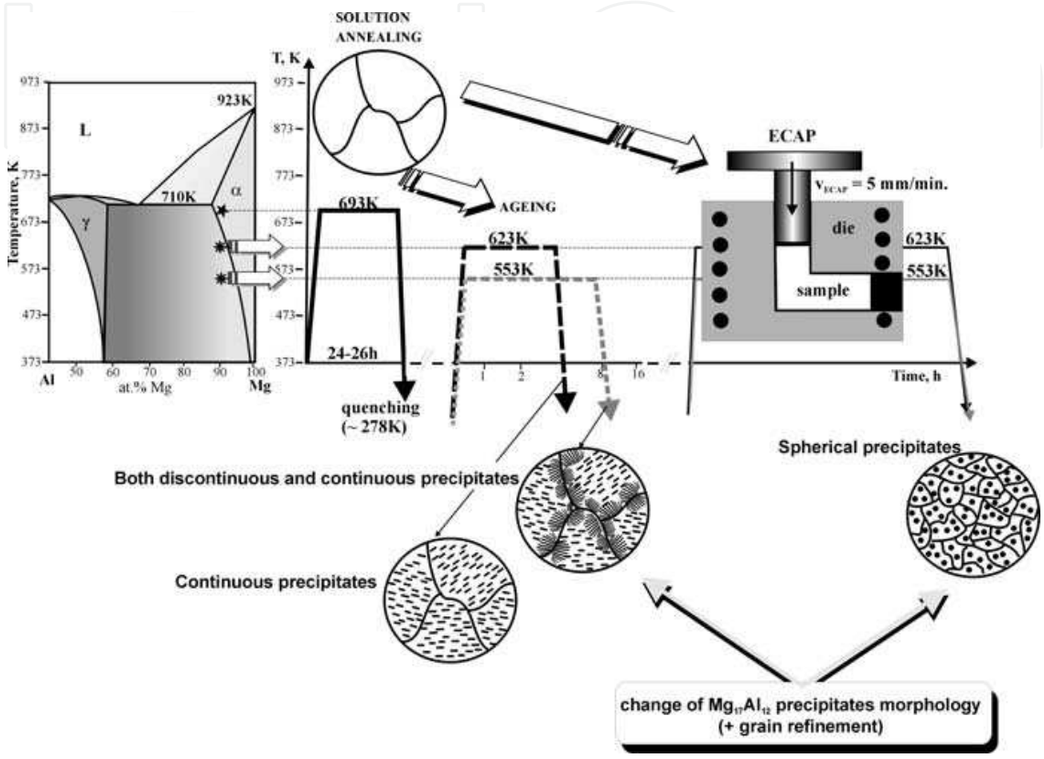

Fig. 15. Scheme of obtained results

8. References

Amir, Q.M. & Gupta, S.P. (1995). Cellular precipitation and precipitate coarsening in a Mg-Al alloy, Canadian Metallurgical Quarterly, Vol. 34, Issue 1, (January 1995) pp. 43-50, ISSN: 00084433

ASM Handbook Committee (1986). Binary alloys phase diagrams, Metals Park, ISBN: 0-87170-261-4, Ohio

Bettles C.J. (2003). The effect of gold additions on the ageing behavior and creep properties of the magnesium alloy AZ91E, Materials Science and Engineering A, Vol. 348, Issue 1-2, (May 2003) pp. 280-288, ISSN 09215093

Bradai D., Kadi-Hanifi M., Zięb, P.. Kuschke W. M. & Gust W. (1999) The kinetics of the discontinuous precipitation and dissolution in Mg-rich Al alloys, Journal of Materials Science, Vol: 34, Issue 21, (November 1999) pp. 5331 – 5336, ISSN 0022-2461

Bradai D., Zieba P., Bischoff E. & Gust W. (2001). A new mode of the discontinuous dissolution reaction in Mg-10 wt.% Al alloy, Materials Chemistry and Physics, Vol. 72, Issue 3, (December 2001) pp. 401-404, ISSN: 02540584

Braszczyńska K.N. (2002). The microstructure of a Mg-10 wt.% Al alloy, Zeitschrift fuer Metallkunde, Vol. 93, Issue 8,(August 2002) pp. 845-850, ISSN: 00443093

Braszczyńska-Malik K.N. (2005). The study on the shaping of the microstructure of magnesium-aluminium alloys, Publisher: WIPMiFS PCz., ISBN 83-87745-72-3, Częstochowa *(in Polish)*

Braszczyńska-Malik K.N. (2009 a). Discontinuous and continuous precipitation in magnesium-aluminium type alloys, Journal of Alloys and Compounds, Vol. 477, Issue 1-2, (May 2009) pp. 870-876, ISSN 0925-8388

Braszczyńska-Malik K.N. (2009 b). Spherical shape of γ-$Mg_{17}Al_{12}$ precipitates in AZ91 magnesium alloy processed by equal-channel angular pressing, Journal of Alloys and Compounds, Vol. 487, Issues 1-2, (November 2009) pp. 263-268, ISSN 0925-8388

Braszczyńska-Malik K.N. & Froyen L. (2005). Microstructure of AZ91 alloy deformed by equal channel angular pressing, Zeitschrift fuer Metallkunde, Vol. 96, Issue 8, (August 2005) pp. 913-917, ISSN: 00443093

Braszczyńska-Malik K.N., Lityńska L. & Baliga W. (2006) Transmission electron microscopy investigations of AZ91 alloy deformed by equal-channel angular pressing, Journal of microscopy, Vol. 224, (October 2006) pp. 15-17, ISSN 0022-2720

Braszczyńska-Malik. K.N., Zawadzki I., Walczak W. & Braszczyński J. (2008). Mechanical properties of high-pressure sie casting AZ91 magnesium alloy, Archives of Foundry Engineering, Vol. 8, Issue 4, (October-December 2008) pp. 15-18, ISSN 1897-3310

Braszczyńska-Malik K.N. & Zyska A. (2010). Influence of solidification rate on microstructure of gravity cast AZ91 magnesium alloy, Archives of Foundry Engineering, Vol. 10, Issue 1, (January-March 2010) pp. 23-26, ISSN 1897-3310

Bursik J. & Svoboda M. (2002). A HREM and Analytical STEM Study of Precipitates in an AZ91 Magnesium Alloy, Microchimica Acta, Vol. 139, Issue 1-4, 39-42, ISSN 0026-3672

Celotto S. (2000). TEM study of continuous precipitation in Mg–9 wt%Al–1 wt%Zn alloy , Acta Matrialia, Vol. 48, Issue 8, (May, 2000) pp. 1775-1787, ISSN 1359-6454

Celotto S. & Bastow T.J. (2001). Study of precipitation in aged binary Mg–Al and ternary Mg–Al–Zn alloys using ^{27}Al NMR spectroscopy, Acta Materialia, Vol. 78, Issue 5, (November 1998), 1137-1149, ISSN1359-6454

Cerri E. & Barbagallo S. (2002). The influence of high temperature exposure on aging kinetics of a die cast magnesium alloys, Mater Letters, Vol. 56, No. 5, (November 2002) pp. 716-720, ISSN 0167577X

Chen B., Lin D-L., Jina L., Zeng X-Q. & Chen L. (2008). Equal-channel angular pressing of magnesium alloy AZ91 and its effects on microstructure and mechanical properties, Materials Science and Engineering A, Vol. 483-484, Issue 1-2 C, (June 2008) pp. 113-116, ISSN: 09215093

Christian J.W. & Mahajan S. (1995). Deformation twinning, Progress in Materials Science, Vol. 39, Issue 1-2, (1995) pp. 1-157, ISSN: 00796425

Duly D, Cheynet MC, & Brechet Y. (1995) On the competition between continuous and discontinuous precipitations in binary Mg-Al alloys, Acta Metallurgica et Materialia, Vol. 43, Issue 1, (January 1995) pp. 101-106, ISSN: 1359-6454

Figueiredo R.B. & Langdon T.G. (2009). Principles of grain refinement and superplastic flow in magnesium alloys processed by ECAP, Materials Science and Engineering A, Vol. 501, Issue 1-2, (February 2009) pp. 105-114, ISSN: 09215093

Gharghouri M.A., Weatherly G.C. & Embury D.J. (1998). The interaction of twins and precipitates in a Mg-7.7at.% Al alloy, Philosophical Magazine A; Vol. 78, Issue 5, (November 1998) pp. 1137-1149, ISSN 01418610

González-Martínez R., Göken J., Letzig D., Steinhoff K., Kainer K.U. (2007). Influence of aging on damping of the magnesium–aluminium–zinc series, Journal of Alloys and Compounds, Vol. 437, Issue 1-2, (June, 2007) pp.127-132, ISSN 0925-8388

Janecek M. & Popov M., Krieger M.G., Hellmig R.J. & Estrin Y. (2007). Mechanical properties and microstructure of a Mg alloy AZ31 prepared by equal-channel angular pressing, Materials Science and Engineering A, Vol. 462, Issue 1-2, (July 2007) pp. 116-120, ISSN: 09215093

Jiang L., Perez-Prado M.T., Gruber P.A., Arzt E., Ruano O.A. & Kassner M.E. (2008). Texture, microstructure and mechanical properties of equiaxed ultrafine-grained Zr fabricated by accumulative roll bonding, Acta Materialia, Vol. 56, Issue 6, (April 2008) pp. 1228-1242, ISSN: 13596454

Koike J., Kobayashi T., Mukai T., Wanatabe H., Suzuki M., Maruyama K. & Higashi K. (2003) The activity of non-basal slip systems and dynamic recovery at room temperature in fine-grained AZ31B magnesium alloys, Acta Materialia, Vol. 51, Issue 7, (April 2003) pp. 2055-2065, ISSN: 13596454

Kulyasova O., Islamgaliev R., Mingler B. & Zehetbauer M. (2009). Microstructure and fatigue properties of the ultrafine-grained AM60 magnesium alloy processed by equal-channel angular pressing, Materials Science and Engineering A, Vol. 503, Issue 1-2, (March 2009) pp. 176-180, ISSN: 09215093

Maîtrejean S., Verona M., Bréchet Y. & Prudy G.R. (1999). Morphological instabilities in Mg-7.7 at % Al, Scripta Materialia, Vol. 41, Issue 11 (November 1999) pp. 1235-1240, ISSN: 13596462

Máthis K., Gubicza J. & Nam N.H. (2005). Microstructure and mechanical behavior of AZ91 Mg alloy processed by equal channel angular pressing, Journal of Alloys and Compounds, Vol. 394, Issue 1-2, (May 2005) pp. 194-199, ISSN: 09258388

Máthis K., Nyilas K. & Axt A. (2004). The evolution of non-basal dislocations as a function of deformation temperature in pure magnesium determined by X-ray diffraction, Acta Materialia, Vol. 52, Issue 10, (June 2004) pp. 2889-2894, ISSN: 13596454

Mordike B. & Ebert T. (2001). Magnesium properties-applications-potential, Materials Science and Engineering A; Vol. 302, Issue 1, (April 15, 2001) pp. 37-45, ISSN 0921-5093

Moreau G., Cornet J. & Calais D. (1971). Acceleration de la diffusion chimique sous irradiation dans le systeme aluminium-magnesium, Journal of Nuclear Materials, Vol. 38, Issue 2, (February 1971) pp.197-202, ISSN: 00223115

Nie J. (2003). Effects of precipitate shape and orientation on dispersion strengthening in magnesium alloys, Scripta Materialia, Vol, 48, Issue 8, (14 April 2003) pp. 1009-1015, ISSN 13596462

Nie J.F., Xiao X.L., Luo C.P. & Muddle B.C. (2001). Characterization of precipitate phases in magnesium alloys using electron microdiffraction, Micron, Vol. 32, Issue 8, (2001) pp. 857-863, ISSN: 09684328

Ohno M., Mirkovic D. & Schmid-Fetze R. (2006), Liquidus and solidus temperatures of Mg-rich Mg–Al–Mn–Zn alloys, Acta Materialia, Vol. 54, Issue 15, (September 2006) pp. 3883-3891, ISSN: 13596454

Ravi Kumar N.V., Blandin J.J., Desrayaund C., Montheillet F. & Surey M. (2003) Grain refinement in AZ91 magnesium alloy during thermomechanical processing, Materials Science and Engineering A, Vol. 359, Issue 1-2, (October 2003) pp. 150-157, ISSN: 09215093

Saito Y., Utsonomiya H., Tsuji N. & Sakai T. (1999). Novel ultra-high straining process for bulk materials development of the accumulative roll-bonding (ARB) process, Acta Materialia, Vol. 47, Issue 2, (January, 1999) pp. 579-583, ISSN: 13596454

Smola B., Stulikova I., von Buch F. & Mordike B.L. (2002). Structural aspects of high performance Mg alloys design. Materials Science and Engineering A; Vol. 324, Issue 1-2, (February, 2002) pp. 113-117, ISSN 0921-5093

Su C.W., Lu L. & Lai M.O. (2006). A model for the grain refinement mechanism in equal channel angular pressing of Mg alloy from microstructural studies, Materials Science and Engineering A, Vol. 434, Issue 1-2, (October 2006) pp. 227-236, ISSN: 09215093

Valiev R.Z., Islamgaliev R.K., & Alexandrov I.V. (2000) Bulk nanostructured materials from severe plastic deformation, Progress in Materials Science, Vol. 45, Issue 2, (March 2000), pp. 103-189, ISSN: 00796425

Valiev R.Z. & Langdon T.G. (2006). Principles of equal-channel angular pressing as a processing tool for grain refinement, Progress in Materials Science, Volume 51, Issue 7, (September 2006) pp. 881-981, ISSN: 00796425

Wang X-S., Jin L., Li Y. & Guo X-W. (2008). Effect of equal channel angular extrusion process on deformation behaviors of Mg-3Al-Zn alloy, Mater Letters, Vol. 62, Issue 12-13, (April 2008) pp. 1856-1858, ISSN: 0167577X

Woo C.H. (2000). Defect accumulation behaviour in hcp metals and alloys, Journal of Nuclear Materials, Vol. 276, Issue 1, (January 2000) pp. 90-103 , ISSN: 00223115

Yoo M.H., Agnew S.R., Morris J.R. & Ho K.M. (2001). Non-basal slip systems in HCP metals and alloys: Source mechanisms, Materials Science and Engineering A, Vol. 319-321, (December 2001) pp. 87-92, ISSN: 09215093

Zhang M.X. & Kelly P.M. (2003). Crystallography of $Mg_{17}Al_{12}$ precipitates in AZ91D alloy, Scripta Materialia, Vol. 48, Issue 5, (March 2003) pp. 647-652, ISSN 13596462

Zhilyaev A.P. & Langdon T.G. (2008). Using high-pressure torsion for metal processing: Fundamentals and applications, Progress in Materials Science, Vol. 53, Issue 6, (August 2008) pp. 893-979, ISSN: 00796425

Zhilyaev A.P., Nurislamova G.V., Kim B.K., Baro M.D. , Szpunar J.A. & Langdon T.G. (2003). Experimental parameters influencing grain refinement and microstructural

evolution during high-pressure torsion, Acta Materialia, Vol. 51, Issue 3, (February 2003) pp. 753-765, ISSN: 13596454

Zięba P. (2000). Recent progress in the energy-dispersive X-ray spectroscopy microanalysis of the discontinuous precipitation and discontinuous dissolution reactions, Materials Chemistry and Physics, Vol. 62, Issue: 3, (February 2000) pp. 183-213, ISSN: 0254-0584

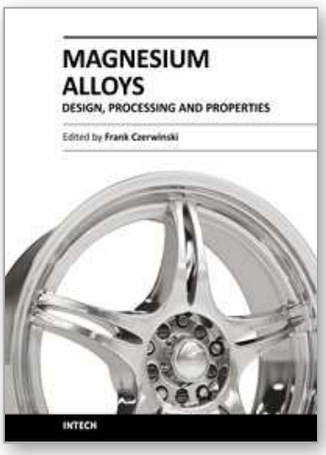

Magnesium Alloys - Design, Processing and Properties

Edited by Frank Czerwinski

ISBN 978-953-307-520-4
Hard cover, 526 pages
Publisher InTech
Published online 14, January, 2011
Published in print edition January, 2011

Scientists and engineers for decades searched to utilize magnesium, known of its low density, for light-weighting in many industrial sectors. This book provides a broad review of recent global developments in theory and practice of modern magnesium alloys. It covers fundamental aspects of alloy strengthening, recrystallization, details of microstructure and a unique role of grain refinement. The theory is linked with elements of alloy design and specific properties, including fatigue and creep resistance. Also technologies of alloy formation and processing, such as sheet rolling, semi-solid forming, welding and joining are considered. An opportunity of creation the metal matrix composite based on magnesium matrix is described along with carbon nanotubes as an effective reinforcement. A mixture of science and technology makes this book very useful for professionals from academia and industry.

INTECH
open science | open minds

InTech Europe
University Campus STeP Ri
Slavka Krautzeka 83/A
51000 Rijeka, Croatia
Phone: +385 (51) 770 447
Fax: +385 (51) 686 166
www.intechopen.com

InTech China
Unit 405, Office Block, Hotel Equatorial Shanghai
No.65, Yan An Road (West), Shanghai, 200040, China
中国上海市延安西路65号上海国际贵都大饭店办公楼405单元
Phone: +86-21-62489820
Fax: +86-21-62489821

IntechOpen